# Development of a population pharmacokinetic model to predict brain distribution and dopamine D2 receptor occupancy of raclopride in non-anesthetized rat

Yin Cheong Wong, Trayana Ilkova, Rob C. van Wijk, Robin Hartman, Elizabeth C.M. de Lange*

*Division of Pharmacology, Cluster Systems Pharmacology, Leiden Academic Center for Drug Research, Leiden University, Leiden, The Netherlands*

## ARTICLE INFO

## ABSTRACT

*Background:* Raclopride is a selective antagonist of the dopamine D2 receptor. It is one of the most frequently used *in vivo* D2 tracers (at low doses) for assessing drug-induced receptor occupancy (RO) in animals and humans. It is also commonly used as a pharmacological blocker (at high doses) to occupy the available D2 receptors and antagonize the action of dopamine or drugs on D2 in preclinical studies. The aims of this study were to comprehensively evaluate its pharmacokinetic (PK) profiles in different brain compartments and to establish a PK-RO model that could predict the brain distribution and RO of raclopride in the freely moving rat using a LC − MS based approach.

*Methods:* Rats (n = 24) received a 10-min IV infusion of non-radiolabeled raclopride (1.61 μmol/kg, *i.e.* 0.56 mg/kg). Plasma and the brain tissues of striatum (with high density of D2 receptors) and cerebellum (with negligible amount of D2 receptors) were collected. Additional microdialysis experiments were performed in some rats (n = 7) to measure the free drug concentration in the extracellular fluid of the striatum and cerebellum. Raclopride concentrations in all samples were analyzed by LC − MS. A population PK-RO model was constructed in NONMEM to describe the concentration-time profiles in the unbound plasma, brain extracellular fluid and brain tissue compartments and to estimate the RO based on raclopride-D2 receptor binding kinetics.

*Results:* In plasma raclopride showed a rapid distribution phase followed by a slower elimination phase. The striatum tissue concentrations were consistently higher than that of cerebellum tissue throughout the whole experimental period (10 − h) due to higher non-specific tissue binding and D2 receptor binding in the striatum. Model-based simulations accurately predicted the literature data on rat plasma PK, brain tissue PK and D2 RO at different time points after intravenous or subcutaneous administration of raclopride at tracer dose (RO < 10%), sub-pharmacological dose (RO 10% − 30%) and pharmacological dose (RO > 30%).

*Conclusion:* For the first time a predictive model that could describe the quantitative *in vivo* relationship between dose, PK and D2 RO of raclopride in non-anesthetized rat was established. The PK-RO model could facilitate the selection of optimal dose and dosing time when raclopride is used as tracer or as pharmacological blocker in various rat studies. The LC − MS based approach, which doses and quantifies a non-radiolabeled tracer, could be useful in evaluating the systemic disposition and brain kinetics of tracers.

## 1. Introduction

Raclopride, a selective dopamine D2 receptor antagonist, is one of the most widely used tracers for the *in vivo* investigations of D2 receptor in animals and humans. In the first reported application of raclopride (Köhler et al., 1985), rats received an intravenous (IV) injection of radiolabeled [3H]-raclopride at a low, tracer dose (2.82 nmol/kg) before the administration of D2 receptor agonists (*e.g.* drugs for

Parkinson's disease) or antagonists (*e.g.* drugs for schizophrenic disorders). The displacement of [3H]-raclopride from the postmortem striatum tissue, the dopaminergic region with high density of D2 receptors, by the drug was measured as receptor occupancy (RO). With the advancement of imaging techniques, raclopride was also applied intravenously to living rats (Hume et al., 1992) and humans (Farde et al., 1986) as radiolabeled [11C]-raclopride for imaging D2 receptors by positron emission tomography (PET).

**Table 1**
Overview of current study and literature reports on single-dose raclopride PK and D2 RO studies in non-anesthetized rats.

| | Current study | (Köhler et al., 1985) | (Suresh et al., 2011) | (Barth et al., 2006) | (Köhler and Karlsson-Boethius, 1988) | (Wadenberg et al., 2000) | (Wadenberg et al., 2000) | (Marcus et al., 2005) |
|---|---|---|---|---|---|---|---|---|
| Rat strain | Wistar | Sprague-Dawley | Sprague-Dawley | Sprague-Dawley | Sprague-Dawley | Sprague-Dawley | Sprague-Dawley | Wistar |
| Body weight, average (kg)[a] | 0.267 | 0.14 | 0.212 | 0.25 | 0.14 | 0.213 | 0.213 | 0.2 |
| Body weight, range (kg) | 0.250–0.285 | 0.13–0.15 | 0.205–0.218 | 0.24–0.26 | 0.13–0.15 | 0.200–0.225 | 0.200–0.225 | 0.18–0.22 |
| Gender | Male | Male | Male | Male | Male | Male | Male | Male |
| Raclopride dose (nmol/kg) | 1613 | 2.82 | 2880 | 6 | 20–3333 | 5760 | 29–5760 | 29–7272 |
| Administration route | IV (10-min infusion) | IV | IV | IV | IV | SC | SC | SC |
| Type of measurement | Plasma PK + brain ECF PK + brain tissue PK + CSF PK | Plasma PK (+ brain tissue PK[b]) | Plasma PK | Brain tissue PK | Striatum D2 RO[c] | Striatum D2 RO[c] | Striatum D2 RO[c] | Striatum D2 RO[d] |
| Number or rats | 24 | NA | 4 | 4 for each time point | 4–6 for each dose | 26 | 23 | 3–6 for each dose |
| Time of measurement | Up to 360 min | Up to 1440 min | Up to 1440 min | Up to 60 min | RO at 75 min | Up to 1440 min | RO at 60 min | RO at 60 min |
| PK profiles presented in | Figs. 2 & 3 | Fig. 4 | Fig. 4 | Fig. 5 | Fig. 6A | Fig. 7B | Fig. 7A | Fig. 7A |

CSF, cerebrospinal fluid; SC, subcutaneous.

[a] The average body weight was used in Berkeley Madonna simulations.

[b] For Köhler et al., 1985, PK was assessed by measuring the total radioactivity in plasma and brain tissue after $^3$H-raclopride dosing. Information regarding the fraction of unchanged raclopride in plasma is available for up to 60 min after IV raclopride dosing (Patel et al., 2008), which is used to convert the total radioactivity to the unchanged raclopride concentration in Fig. 4. Information regarding the fraction of unchanged raclopride in brain tissue is not available, and so the brain tissue data was not further analyzed.

[c] IV $^3$H-raclopride was used as tracer for these in vivo D2 RO studies.

[d] $^{125}$I-iodosulpride was used as tracer for this ex vivo D2 RO study.

Raclopride is also used in higher doses for neurological and behavioral studies in rats. In this case raclopride acts as a D2 blocker to partially or completely occupy the available receptors and prevent the potential interactions between the D2 receptors and the studied drug (and endogenous dopamine), which would verify the role of D2 receptors in the functional outcomes of the interventions. Therefore, the dose of raclopride in rat could range from very low (as tracer) to very high (as pharmacological blocker) depending on the purpose, and choosing an accurate dose is of utmost importance.

While raclopride has been used in rat studies for three decades, surprisingly many crucial aspects of its pharmacokinetics (PK) have remained unknown. Although there were a few studies on the PK of IV raclopride in non-anesthetized rat (Table 1), the utility of those PK data was hampered by the study design employed. First, in one study, for some studies radiolabeled [$^3$H]-raclopride was administered and the total radioactivity in plasma or brain tissue was measured (Köhler et al., 1985). Since raclopride is rapidly metabolized, soon after IV administration the parent raclopride only accounted for a small portion of the total radioactivity in plasma (< 60% at 20 min) (Patel et al., 2008). Therefore, the radioactivity-time profile could not be translated into the raclopride concentration-time profile. Second, in two other studies, plasma and brain tissue PK profiles were not simultaneously reported (Barth et al., 2006; Suresh et al., 2011). Third, there is no report on the free drug concentration in brain extracellular fluid (ECF), which is the driving force for binding to membrane receptors (de Lange, 2013).

To determine the optimal raclopride dose for a particular study, a mathematical model that could link the dose to PK profiles in relevant body compartments and brain D2 RO is needed. A few compartmental PK models have been developed, but all of them were derived from the radioactivity data of PET imaging studies, which were performed in anesthetized rats that received IV [$^{11}$C]-raclopride (Hume et al., 1992; Morris and Yoder, 2007). The predictive power of these models has also not been validated with external data. In addition to the aforementioned problem related to radioactive metabolites, the total radioactivity measured also could not make distinction between brain ECF concentration and brain tissue cell concentration. Moreover, the anesthesia procedures have profound impact on the PK and D2 RO of raclopride. Obviously, non-anesthetized rats are preferred in most neurological studies, especially for those intended to link the drug PK profile to the behavioral and neurochemical changes (Wong and Zuo, 2013). Furthermore, striatum D2 RO should be incorporated in the model since it has been demonstrated that the pharmacological effect of raclopride could be predicted from its RO (Wadenberg et al., 2000). Therefore, there is a need for a new PK-RO model that is derived from data of non-anesthetized rats.

Recently, it is proposed that in small animals the *in vivo* brain kinetics of a tracer could be evaluated with a LC − MS based approach, which doses and quantifies a non-radiolabeled tracer instead of a radiolabeled one (Joshi et al., 2014). The main advantages are the avoidance of the physiological and technical concerns associated with the use of anesthesia and radiotracer in the PET imaging approach, which could facilitate the development of new tracers (details in Discussion Sections 4.2 and 4.3).

The aim of the current study is to develop a model that could predict the PK profiles of raclopride in plasma and brain and the corresponding D2 RO in the striatum. To that end, with a LC − MS based approach, we first performed an *in vivo* study to simultaneously measure raclopride concentrations in plasma, brain ECF (with microdialysis technique) and brain tissue in non-anesthetized, freely moving rats receiving non-radiolabeled raclopride *via* IV administration. The data would be used to construct a PK-RO model with the population approach that took into account the inter-individual variability between the studied rats. The developed model would be validated by comparing the simulated PK and D2 RO values to those reported in previous literature (Table 1). The developed PK-RO model is expected to become a useful tool to guide researchers on the optimal dosing of raclopride in different types of studies.

## 2. Methods

### 2.1. Animals

Animal experiments were performed in accordance with the Dutch Law of Animal Experimentation. The study protocol (DEC14051) was approved by the Animal Ethics Committee in Leiden. Male Wistar rats (n = 24, Charles River, The Netherlands) were housed in groups for 6–9 days until surgery (Animal Facilities Gorlaeus Laboratories, Leiden, The Netherlands), under standard environmental conditions with *ad libitum* access to food (Laboratory chow, Hope Farms, Woerden, The Netherlands) and acidified water. Artificial daylight was provided from 7:30 AM to 7:30 PM. The average weight of the rat was 0.267 ± 0.008 kg on the day of pharmacokinetic experiment. The general setting of the animal experiment was adapted from van den Brink et al. (2017), and the details were outlined below.

### 2.2. Surgery

The surgery was executed as described previously (Westerhout et al., 2012) with small modifications. To summarize, during all surgical procedures the rats were kept under 2% isoflurane anesthesia. Cannulas were placed in the femoral vein for the administration of raclopride and in the femoral artery for blood sampling. In seven rats microdialysis would be performed for serial sampling of brain ECF. In these rats, two microdialysis guides (CMA 12 Guide Cannula, Aurora Borealis Control BV, Schoonebeek, the Netherlands) were embedded in the brain striatum (AP −1.0; L 3.2; V −3.5 mm relative to bregma) and cerebellum (AP −2.51; L 2.04; V −3.34 mm, at an angle of 25° from the dorsoventral axis (toward anterior) and 11° lateral from the anteroposterior axis relative to lambda). The rats were given 7 days to recover from surgery in Makrolon type 3 cages. One day before the experiment, the microdialysis guides were substituted by the microdialysis probes (CMA 12 Elite Polyarylethersulfone, 4 mm membrane, cut-off 20 kDA, Aurora Borealis Control BV, Schoonebeek, the Netherlands).

### 2.3. Pharmacokinetic experiment

The experimental setting of the current study was summarized in Table 1. All experiments started between 8:00 AM and 9:00 AM. Raclopride infusion solution was prepared by dissolving non-radiolabeled S(−)-raclopride (+)-tartrate (Sigma-Aldrich, St Louis, USA) in saline. Rats received 10-min IV infusion of raclopride 0.56 mg/kg (*i.e.* 1612 nmol/kg) at the start of experiment (t = 0 min). Microdialysate perfusion buffer was prepared as described previously (Stevens et al., 2009), and 60 min before the experiment the perfusion was started using a flow rate of 1 μL/min until the end of experiment. Microdialysis samples were collected every 20 min, and those with a deviated flow rate of > 10% were discarded. Blood samples of 200 μL were collected at serial time points in heparin-coated plastic tubes. After each sampling 200 μL saline was injected to compensate the fluid loss. The samples were centrifuged (2300 × *g*, 10 min) for separation of plasma. At a predefined time point after raclopride administration, the rat was euthanized with an overdose of pentobarbital sodium (ASTfarma B.V., The Netherlands) *via* the venous cannula. Cerebrospinal fluid was collected with cisternal puncture before transcardial perfusion with 50 mM phosphate buffer (pH 7.4). The cerebrospinal fluid sample was visually inspected for blood contamination (discarded if contaminated), briefly centrifuged (16,100 × *g*, 1 min), and the bottom portion (≈ 20 μL) was removed since it might contain some large molecules such as blood cells (if any). The whole brain was removed, and the cerebellum and striatum were dissected and weighed. All samples were stored at 4 °C during the experiment and at −80 °C after the experiment until analysis.

### 2.4. Sample analysis

The concentrations of raclopride in the plasma, brain tissue and microdialysate were measured using the liquid-liquid extraction and LC-MS/MS assay methods previously developed and validated in our laboratory (Stevens et al., 2010) with small modifications. In short, formic acid instead of trifluoroacetic acid was added to the solvents of on-line solid phase extraction and liquid chromatography to improve the column lifetime while maintaining the same performance in peak shape and resolution. Moreover, raclopride-d5 (Toronto Research Chemicals Inc., Toronto, Canada) was used as the internal standard. Cerebrospinal fluid was analyzed in the same manner as that of microdialysate. The lower limits of quantification of plasma, brain tissue, microdialysate and cerebrospinal fluid were 3.6 nM, 2.8 nM, 1 nM and 1 nM, respectively. Samples with concentrations lower than the lower limit of quantification were excluded from the PK-RO modeling.

The *in vivo* recovery of the microdialysis probe was determined by *in vivo* loss experiments (Yamamoto et al., 2017) by perfusing the probe with raclopride at 58, 288, and 864 nM. The recoveries of striatum probe (28 ± 4%) and cerebellum probe (28 ± 4%) were found to be the same. Therefore, the microdialysate concentrations in both tissues were corrected for 28% to obtain the brain ECF concentrations. The total plasma concentrations were corrected for the fraction unbound of 36.7% (Summerfield et al., 2008) to obtain the unbound plasma concentration.

### 2.5. Development and evaluation of the population PK-RO model

The population PK-RO analysis was performed using a non-linear mixed effects modeling approach, which estimates the typical (mean) value of model parameters as well as their inter-individual variances. In NONMEM® (version 7.3.0, ICON), subroutine ADVAN6 and first-order conditional estimation with interaction (FOCE-I) method were used to estimate the model parameters. Exponential error models were utilized to estimate the inter-individual variability in parameters. For residual unexplained variability, proportional and additive plus proportional models were tested. The stability of the model was assessed on the basis of goodness of fit plots and successful termination with estimates of fixed effects not close to a boundary. The robustness of the final model was assessed by bootstrap. Predictive checks were also performed by overlaying the model-based simulations and the observed concentrations to evaluate the predictability of the model (Bosch et al., 2016). The model structure is shown in Fig. 1. The differential equations are listed in Table 2.

Regarding the raclopride-D2 binding in striatum, the association rate $k_{on}$ at 0.049 $nM^{-1} min^{-1}$ and the dissociation rate $k_{off}$ at 0.078 $min^{-1}$ were used as initial estimates, which corresponded to an affinity $K_d$ (= $k_{off}$ / $k_{on}$) of 1.6 nM. These values were obtained from *in vitro* raclopride binding kinetics assays on D2 receptors expressed on CHO-cells (Packeu et al., 2010), and similar values were also observed in *in vitro* assays with rat striatum homogenate (Hall et al., 1988). The concentration of total D2 binding site in striatum ($B_{max}$) was fixed to 25 nM (Cumming, 2011; Hall et al., 1988).

### 2.6. Simulation in Berkeley Madonna and comparison with literature data

Simulations were performed using the differential equation solver in the Berkeley Madonna software (Version 8.3.18), with the fourth-order Runge-Kutta integration algorithm. To simulate the drug concentrations and D2 RO outcomes after IV raclopride dosing, the estimated parameters of the structural model (Table 3) were used while the variabilities (inter-individual variability and residual unexplained variability) were not incorporated in the simulation. Allometric scaling of systemic drug disposition was necessary since in previous studies the body weights of the rats differed widely (Table 1). The systemic clearance from central distribution compartment (*V1*) of the rat in a
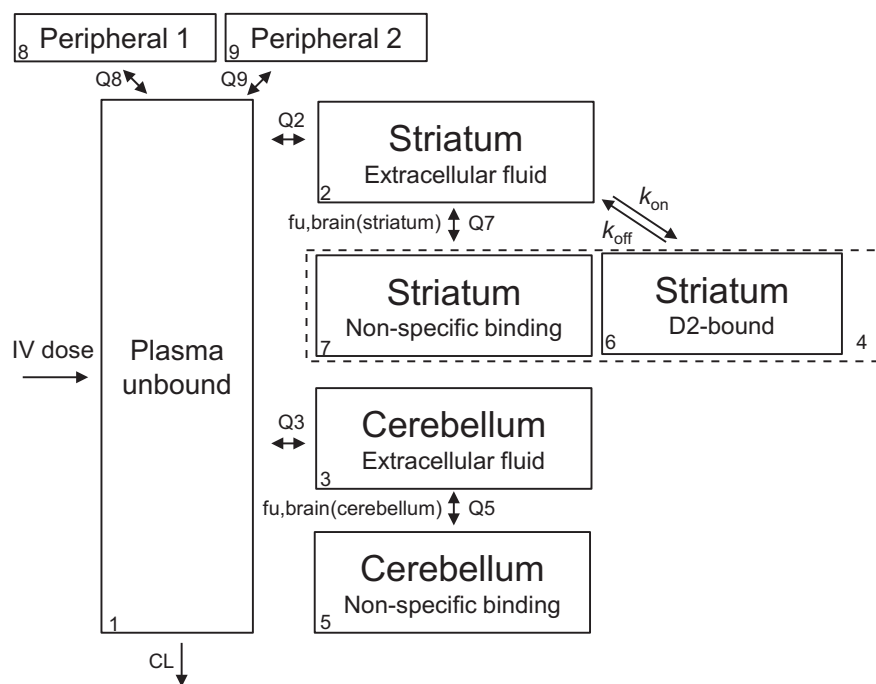
**Fig. 1.** Schematic overview of the PK-RO model describing the concentration-time profiles of raclopride in plasma and brain.

previous study ($CL_{new}$) was derived from the systemic clearance in the current PK-RO model ($CL_{original}$, *i.e.* 0.0426 L/min), such that $CL_{new} = CL_{original} \times (BW_{new}/BW_{original})^{exp}$, where $BW_{new}$ and $BW_{original}$ were the average body weights of the rats in that previous study and in the current study (0.267 kg), respectively. The central distribution compartment ($V1$) and the two peripheral distribution compartments ($V8$ and $V9$) were also scaled in the same way. The exponents ($exp$) for clearance and distribution volumes were 0.75 and 1, respectively (Knibbe et al., 2005). Allometric scaling was not performed for the brain compartments since starting from the age of one month (body weight around 0.08 kg) the volume of brain is already close to (around 90%) that of full adult (Mengler et al., 2014). To further simulate the RO outcome after subcutaneous raclopride dosing, an absorption process from the subcutaneous site to plasma was added to the differential equations and was described by a first-order absorption rate. All simulations were then compared to the observed data obtained from previous studies (Table 1).

**Table 2**
Differential equations for the PK-RO model.

| Compartment number and equation | Explanation |
|---|---|
| 1. d/dt (A1) = − K ∗ A1 − K12 ∗ A1 + K21 ∗ A2 − K13 ∗ A1 + K31 ∗ A3 − K18 ∗ A1 + K81 ∗ A8 − K19 ∗ A1 + K91 ∗ A9 + rate_in | • Unbound plasma compartment |
| 2. d/dt (A2) = K12 ∗ A1 − K21 ∗ A2 − K27 ∗ A2 + K72 ∗ A7 ∗ FUST − KON ∗ A2 / V2 ∗ (TotalAD2 − A6) + KOFF ∗ A6 | • Brain striatum extracellular fluid (ECF) compartment [measured by microdialysis] |
| 3. d/dt (A3) = K13 ∗ A1 − K31 ∗ A3 − K35 ∗ A3 + K53 ∗ A5 ∗ FUCB | • Brain cerebellum extracellular fluid (ECF) compartment [measured by microdialysis] |
| 4. d/dt (A4) = A6 + A7 | • Brain tissue striatum, total amount of raclopride (D2-bound plus non-specific tissue bound, *i.e.* A6 + A7) [measured by total tissue homogenate] |
| 5. d/dt (A5) = K35 ∗ A3 − K53 ∗ A5 ∗ FUCB | • Brain tissue cerebellum, total amount of raclopride (D2-bound plus non-specific tissue bound; but negligible amount of D2 receptor in cerebellum assumed) [measured by total tissue homogenate] |
| 6. d/dt (A6) = KON ∗ A2/V2 ∗ (TotalAD2 − A6) − KOFF ∗ A6 | • Brain tissue striatum, amount of D2-bound raclopride (A6: amount of D2-raclopride complex) |
| 7. d/dt (A7) = K27 ∗ A2 − K72 ∗ A7 ∗ FUST | • Brain tissue striatum, amount of non-specific tissue bound raclopride |
| 8. d/dt (A8) = K18 ∗ A1 − K81 ∗ A8 | • Peripheral compartment 1 |
| 9. d/dt (A9) = K19 ∗ A1 − K91 ∗ A9 | • Peripheral compartment 2 |

FUCB: fraction unbound in cerebellum tissue; FUST: fraction unbound in striatum tissue.
rate_in: rate of raclopride entrance into unbound plasma compartment (nmol min$^{-1}$).
TotalAD2 = total amount of D2 receptor binding site in striatum tissue (nmol), *i.e.* total concentration of D2 receptor binding site in striatum ($B_{max}$ = 25 nM) × physiological volume of striatum (0.0001 L) = 0.0025 nmol.

**Table 3**
Parameter estimates and bootstrap results for the raclopride PK-RO model.

| Parameter | Unit | Parameter estimate | RSE | Bootstrap median[a] | CV |
|---|---|---|---|---|---|
| **Structural model** | | | | | |
| CL | L/min | 0.0426 | 3.9% | 0.0431 | 4.0% |
| V1 | L | 0.0255 | 15.9% | 0.0269 | 20.9% |
| Q2 | L/min | 0.0281 | 13.9% | 0.0266 | 30.0% |
| V2 | L | 0.405 | 14.1% | 0.400 | 31.9% |
| Q3 | L/min | 0.0169 | 14.7% | 0.0199 | 38.0% |
| V3 | L | 0.205 | 24.3% | 0.218 | 49.7% |
| fu,brain (striatum) | | 0.0970 | 6.1% | 0.0965 | 8.0% |
| fu,brain (cerebellum) | | 0.130 | 10.7% | 0.128 | 11.4% |
| $k_{off}$ | min$^{-1}$ | 0.165 | 20.4% | 0.161 | 35.7% |
| $k_{on}$ | nM$^{-1}$ min$^{-1}$ | 0.049 | (fixed) | N.A. | N.A. |
| Q5 | L/min | 0.06 | (fixed) | N.A. | N.A. |
| V5 | L | 0.0002[b] | (fixed) | N.A. | N.A. |
| V6 | L | 0.0001[b] | (fixed) | N.A. | N.A. |
| Q7 | L/min | 0.06 | (fixed) | N.A. | N.A. |
| V7 | L | 0.0001[b] | (fixed) | N.A. | N.A. |
| Q8 | L/min | 0.0035 | (fixed) | N.A. | N.A. |
| V8 | L | 1.24 | (fixed) | N.A. | N.A. |
| Q9 | L/min | 0.0595 | (fixed) | N.A. | N.A. |
| V9 | L | 0.146 | (fixed) | N.A. | N.A. |
| **Inter-individual variability (IIV)** | | | | | |
| IIV-CL | | 0.0321 | 29.3% | 0.0308 | 45.1% |
| IIV-Q3 | | 0.0504 | (fixed) | N.A. | N.A. |
| IIV-V3 | | 0.0648 | (fixed) | N.A. | N.A. |
| IIV-Q9 | | 0.128 | (fixed) | N.A. | N.A. |
| **Proportional residual variability** | | | | | |
| Plasma[c] | | 0.0173 (4.0)[c] | 24.9% (22.4%)[c] | 0.0164 (4.0)[c] | 27.7% (20.7%)[c] |
| Striatum ECF | | 0.0572 | 19.2% | 0.0527 | 28.0% |
| Cerebellum ECF | | 0.0404 | 21.4% | 0.0404 | 25.2% |
| Striatum tissue | | 0.0240 | 52.9% | 0.0215 | 85.1% |
| Cerebellum tissue | | 0.0880 | 37.2% | 0.0796 | 40.5% |

RSE = relative standard error. CV = coefficient of variation.

[a] Based on 157 bootstrap runs that minimized successfully.

[b] The volume of cerebellum tissue (V5) and striatum tissue (V6 and V7) was fixed to the physiological volume (200 mg and 100 mg, approximately 0.0002 L and 0.0001 L, respectively).

[c] Combined proportional and additive error was used for plasma compartment.

## 3. Results

### 3.1. In vivo microdialysis study: characteristics of raclopride PK profiles after IV dosing

The PK profiles in plasma, brain ECF and tissues after the 10-min IV raclopride infusion are presented in Fig. 2. For the first 3 h, raclopride showed a biphasic decline in plasma with a rapid distribution phase (lasted for around 20 min after the infusion) and a slower elimination phase. Indeed, our simulation suggested that 3 h after the dosing there would be a third phase in which the plasma elimination rate became even slower (Fig. 4). For brain ECF, the PK profiles in striatum and cerebellum were similar, and both demonstrated monophasic elimination for the first 2.5 h. For brain tissues, the elimination of raclopride was biphasic and the elimination rate became slower at time = 4 h. Concentrations in striatum tissue were consistently higher than that of cerebellum tissue throughout the whole experimental period (10-h) in each studied rat. The concentration in cerebrospinal fluid was similar to those in ECF (Supplementary Fig. 1).
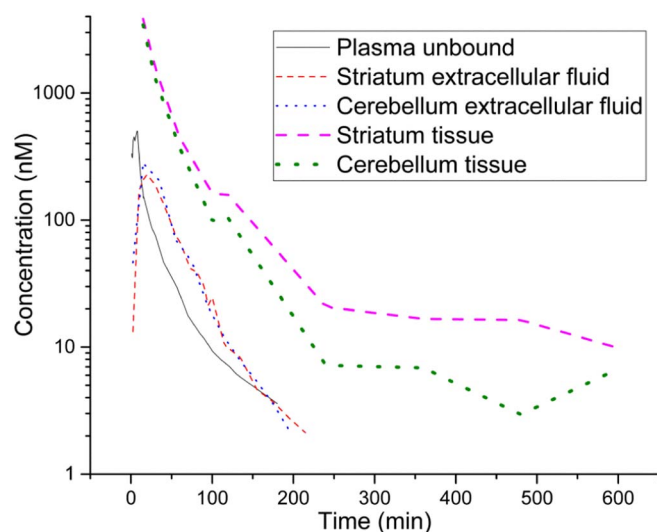


**Fig. 2.** PK profiles of raclopride in different compartments after IV raclopride dosing (1613 nmol/kg). The curves are generated by local regression smoothing (LOESS). The scatterplots for the data of each compartment are shown in Fig. 3A to E.

### 3.2. Development of the PK-RO model

The model structure is shown in Fig. 1. Before incorporating the brain compartments, we first developed a simple PK model that could adequately describe the plasma PK profile. Adding one peripheral distribution compartment to the central compartment made it possible for NONMEM to describe the plasma data in NONMEM, but the addition of a second peripheral compartment was even better in terms of objective function values. Further addition of peripheral compartments did not significantly improve the model. In addition to an improvement in objective function values, our simulation based on a PK model with two peripheral compartments also adequately captured the tri-phasic PK profile of non-radiolabeled raclopride observed in (Suresh et al., 2011) (Fig. 4). Therefore, a PK model consisted of a central compartment and two peripheral compartments was adopted. While the exact pharmacological mechanisms that give rise to two peripheral compartments remain to be explored, it is possible that one peripheral compartment (compartment 8) represents the body tissues that the lipophilic raclopride has high affinity to but the blood perfusion to these tissues is poor (e.g. lipophilic tissues such as fat tissue). This would manifest as a high volume of distribution (high V8 of 1.24 L) but low clearance (low Q8 of 0.0035 L/min) as shown in Table 3. On the other hand, the other peripheral compartment (compartment 9) might represent the body tissues that the lipophilic raclopride has low affinity to but the blood perfusion to these tissues is good.

Considering the complexity of the PK-RO model, certain constraints had to be applied to the model to enhance the sensitivity of the model to the remaining parameters and to reduce the uncertainty in their estimation. The main constraints applied were (1) the clearance between brain ECF and brain cells (Q5 and Q7) was fixed at a high arbitrary value, (2) certain PK parameters were fixed in the final PK-RO model, and (3) $k_{on}$ was fixed at the value reported in in vitro binding kinetics study and $k_{off}$ was estimated by the PK-RO model. The rationales behind these constraints are explained below in Section 3.2.

Raclopride can rapidly penetrate across the biological membranes. In vitro studies suggest that for raclopride the entire process of phospholipid membrane translocation (from drug adsorption to membrane to drug release from membrane) could occur on a time scale of seconds (Baciu et al., 2006; Casey et al., 2014). Therefore, a fast equilibrium between brain ECF and brain cells was assumed, and the clearance

between these two compartments (Q5 and Q7) was artificially fixed at a high value. Sensitivity analysis suggested that the estimation of other parameters was not sensitive to the value of Q5 and Q7 (unless Q5 and Q7 were at unreasonably low values) (data not shown). Similar approach was also used in the modeling of intra-brain distribution of other lipophilic drugs (Kozielska et al., 2012). The estimated unbound fraction of raclopride in brain ($f_{u,brain}$) was lower in striatum (0.097) than that in cerebellum (0.13). With the *in vitro* brain slice method (Loryan et al., 2013), the unbound volume of distribution of raclopride in striatum and cortex was 11.2 and 9.8 mL per gram of brain tissue, respectively (personal communication with Irena Loryan), which also suggested a higher binding to the striatum tissue. Due to the complexity of the PK-RO model, NONMEM was unable to give stable estimation on the parameters of the peripheral compartments and some parameters related to the inter-individual variability. Therefore, we estimated these parameter with a PK model (without receptor binding), and the estimated values were then fixed in the subsequent PK-RO model.

To model the binding of raclopride to D2 receptors, at first we tried to estimate $k_{off}$ and $k_{on}$ simultaneously. However, during the NONMEM iterations both $k_{off}$ and $k_{on}$ kept increasing monotonically without any sign of convergence while the ratios of $k_{off}$ and $k_{on}$ maintained at around 3.3 to 3.4 at each iteration. The model could not minimize successfully, probably because that based on the available data NONMEM could estimate $K_d$ (*i.e.* $k_{off}/k_{on}$) but not individual $k_{off}$ and $k_{on}$ values. We then tried fixing either the $k_{off}$ value or $k_{on}$ value to the initial estimate ($k_{off}$ at 0.078 $min^{-1}$ or $k_{on}$ at 0.049 $nM^{-1}$ $min^{-1}$, see Section 2.5) and estimating the other. Both models could minimize successfully. When $k_{off}$ was fixed at 0.078 $min^{-1}$, the estimated $k_{on}$ was 0.0228 $nM^{-1}$ $min^{-1}$. On the other hand, when $k_{on}$ was fixed at 0.049 $nM^{-1}$ $min^{-1}$, the estimated $k_{off}$ was 0.165 $min^{-1}$. Therefore, both models gave an estimate of $K_d$ at 3.4 nM. The two models gave exactly the same estimates on all parameters (in both structural model and the variabilities). Nevertheless, the precision of the estimates was much higher when $k_{on}$ was fixed (RSE ≤ 29% for all parameters, except for residual variability in cerebellum tissue and striatum tissue, Table 3) than that when $k_{off}$ was fixed (RSE 37% − 350% for most parameters, data not shown). Since the model with $k_{on}$ fixed and $k_{off}$ estimated gave more a reliable estimation, this model was chosen for further evaluations.

### 3.3. Evaluation of the PK-RO model

Visual predictive check was conducted by performing simulations of the model for 200 times. The PK-RO model showed acceptable predictive performance, and the predictions overlaid the observed concentrations with good agreement in all the five compartments (Fig. 3).

Goodness-of-fit plots for observations *versus* predictions (population predicted and individual predicted) are provided in the Supplementary Fig. 2. No systematic differences between observations and predictions were found, except that for striatum tissue and cerebellum tissue there were a slight underestimation at the highest concentrations which were measured soon after the completion of raclopride IV infusion (t = 15 min). We tried to capture this unexpectedly high concentration by adding a direct clearance between the plasma and brain tissue compartment (Westerhout et al., 2013), but this did not improve the prediction. In the current study, raclopride was administered as a 10-min infusion (of diluted raclopride solution) instead of bolus injection (of concentrated raclopride solution). The reasons were first to reduce the potential changes in physiology and behavior (*e.g.* motor dysfunctions such as catalepsy, (Wadenberg et al., 2000)) induced by this relatively high dose of raclopride and second to enhance the accuracy of the amount of raclopride dosed. No brain tissue samples and only very few brain ECF samples were collected before the completion of the 10-min infusion. Therefore, the data did not have enough information to provide a precise estimate of the initial (rapid) uptake from plasma to brain ECF to brain tissue, and the initial binding from brain ECF to D2

receptors. This might also explain why NONMEM gave less precise estimations when it was asked to estimate the drug association rate to D2 ($k_{on}$) as mentioned above.

The robustness of the model was assessed by bootstrap where the original data were resampled. The model showed a high level of precision and the parameter estimates of the model were similar to that of the bootstrap. Therefore, this model was chosen as the final model, and it was used for subsequently simulations in Berkeley Madonna.

### 3.4. Prediction accuracy of the PK-RO model for IV raclopride administration

The ultimate goal of this project was to predict the raclopride PK and D2 RO in rats on the basis of our PK-RO model. The accuracy of the prediction was evaluated by comparing the simulations generated in Berkeley Madonna to those reported in previous literature (Table 1). The model accurately predicted the plasma PK profiles after a tracer dose (2.82 nmol/kg as [³H]-raclopride) and also a 1000-fold higher dose (2880 nmol/kg as non-radiolabeled raclopride) (Fig. 4). It also predicted the residue level of raclopride remaining in plasma one day after the IV dose, and the two different elimination phases. After a low dose of raclopride (6 nmol/kg), the model captured the trend of raclopride concentration in cerebellum and striatum tissues, although it underestimated the initial, highest concentration in striatum at t = 5 min (Fig. 5), which was a limitation of the model as discussed above. At this sub-pharmacological dose, the maximum D2 RO was estimated to be 18%, which was consistent with the RO value suggested by the investigators of that study (23%, (Barth et al., 2006)). Most importantly, the model predicted well the striatum D2 RO values observed after different IV doses (Köhler and Karlsson-Boethius, 1988) (Fig. 6A), which strongly supported the validity of the model. The effect of changing the $k_{off}$ value from 0.165 $min^{-1}$ (while $k_{on}$ kept constant) on RO was simulated. It could be observed that RO was sensitive to the $k_{off}$ value, and a relatively small, two-fold change in would already result in a considerable shift in the dose-RO curve (Fig. 6B). A simulation example (based on the setting of rat D2 RO studies after IV raclopride by (Köhler and Karlsson-Boethius, 1988)) is provided in Berkeley Madonna code in the Supplementary material.

### 3.5. Prediction accuracy of the PK-RO model for subcutaneous raclopride administration

We tried to extend the application of the PK-RO model, which was based on IV raclopride data, to the prediction in rats receiving subcutaneous dosing. A first-order absorption rate was added to the model to describe absorption process from the subcutaneous site to plasma. Different values for this absorption rate were tested, and it was found that the predicted RO-time profile increasingly approached the observed RO-time profile (Fig. 7B) when the absorption rate kept increasing up to 0.4 $min^{-1}$, while a further increase in absorption rate had no apparent impact on the simulated PK or RO profiles. Therefore, the absorption rate was fixed at 0.4 $min^{-1}$ for subsequent simulations. The model not only predicted the RO after different subcutaneous doses (Fig. 7A), it also predicted the RO at different time points, up to one day after a subcutaneous dose (Fig. 7B). Under this fast absorption rate the simulated plasma PK profile after subcutaneous dosing was similar to that of IV raclopride, and the whole subcutaneous dose was completely absorbed into plasma within a few minutes. Efficient subcutaneous absorption is supported by *in vivo* observations. Even when subcutaneous raclopride was administered to rat at much lower doses of ≤ 288 nmol/kg (20-fold lower compared with the 5760 nmol/kg by (Wadenberg et al., 2000) in Fig. 7B), the D2-blockade-induced effects on behavior (suppression of conditioned avoidance response) and neurotransmitter levels (enhanced dopamine turnover) appeared very soon after subcutaneous administration, before t = 20 min (Linnér et al., 2002).
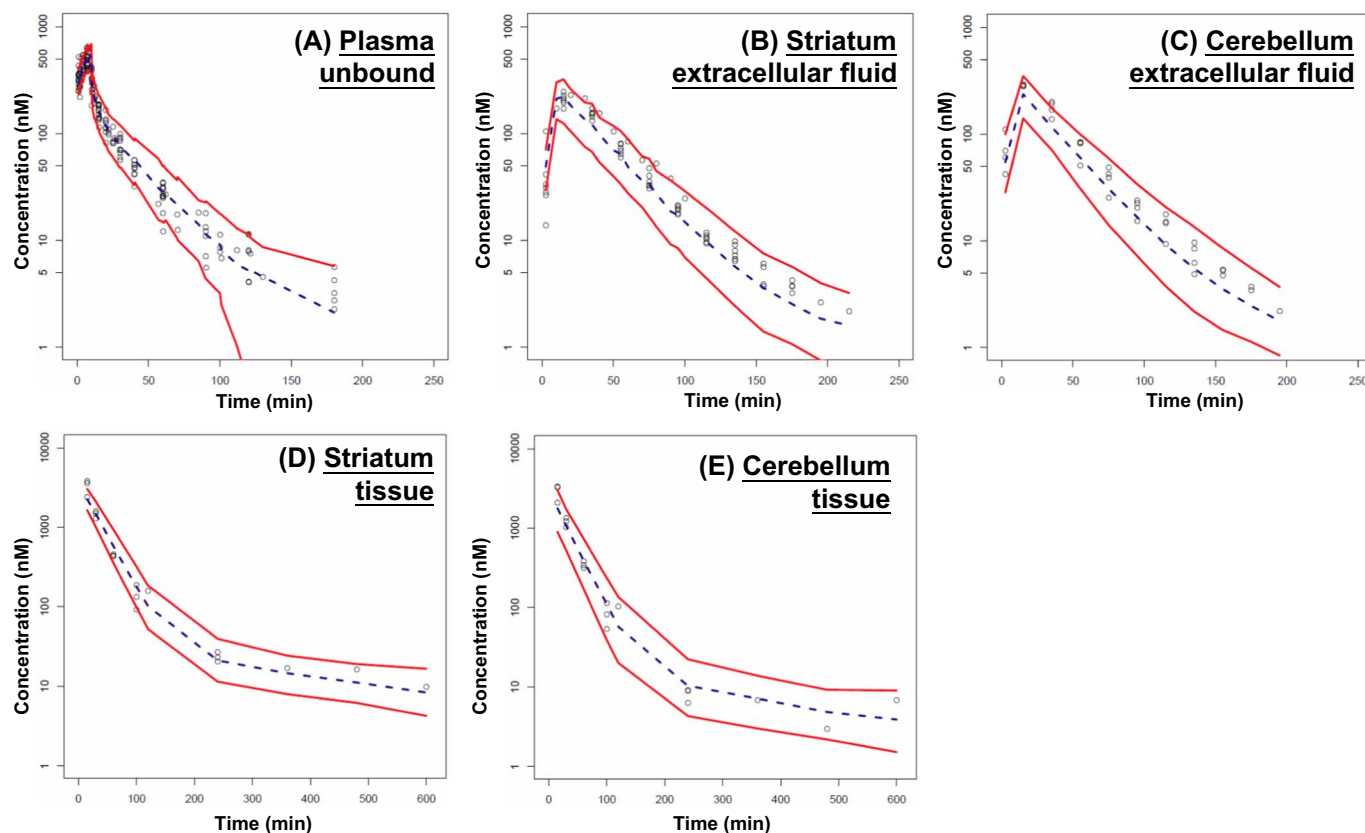
**Fig. 3.** Predictive check of the PK-RO model. Red lines represent 5% and 95% prediction quantile based on 200 simulated datasets. Dotted lines represent median of the simulated data. Dots were observed data from the present study, at raclopride IV dose 1613 nmol/kg. (For interpretation of the references to color in this figure legend, the reader is referred to the web version of this article.)
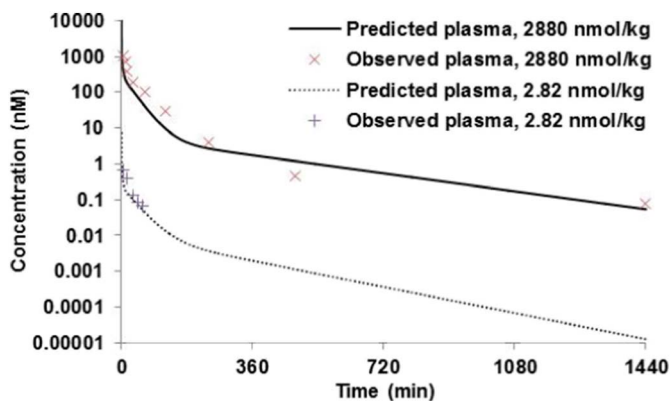


**Fig. 4.** Prediction of unbound plasma PK after IV raclopride administration. Observed data were from Suresh et al. at 2880 nmol/kg, and Köhler et al. at 2.82 nmol/kg.



**Fig. 5.** Prediction of brain tissue PK after IV raclopride. Observed data were from Barth et al. at 6 nmol/kg. The corresponding RO was also simulated.

## 4. Discussion

### 4.1. Novelty of the current study and utility of the developed PK-RO model

To our knowledge, this is the first population model developed for raclopride and it could predict the PK and D2 RO after IV raclopride dosing in rats. By combining the microdialysis technique (for brain ECF measurement), $LC-MS$ quantification and population modeling, quantitative estimation of PK parameters of the non-radiolabeled drug in all relevant plasma and brain compartments became feasible (Yamamoto et al., 2017). Incorporating D2 receptor binding into the PK model makes the model useful for dose selection since the pharmacological effects of raclopride is directly linked to and could be predicted from its striatum RO (Wadenberg et al., 2000). Specifically, in rats
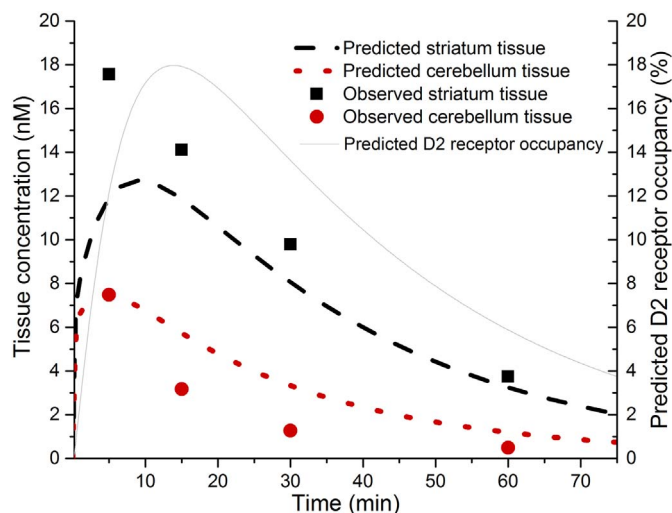
dosed with raclopride, suppression of conditional avoidance response (a tentative behavioral marker suggesting an antipsychotic effect, (Wadenberg, 2010)) occurs at a D2 RO around $70-75\%$ while catalepsy (a tentative behavioral marker suggesting motor dysfunction side effect, (Wong and Zuo, 2013)) emerges only when D2 RO is > 80% (Wadenberg et al., 2000). In addition to predicting the RO after IV raclopride (Fig. 6), the model could be extended to predict the RO after subcutaneous raclopride administration (Fig. 7). Nevertheless, the validity of this tentative subcutaneous model should be further verified with plasma (and brain) PK data from rats receiving subcutaneous
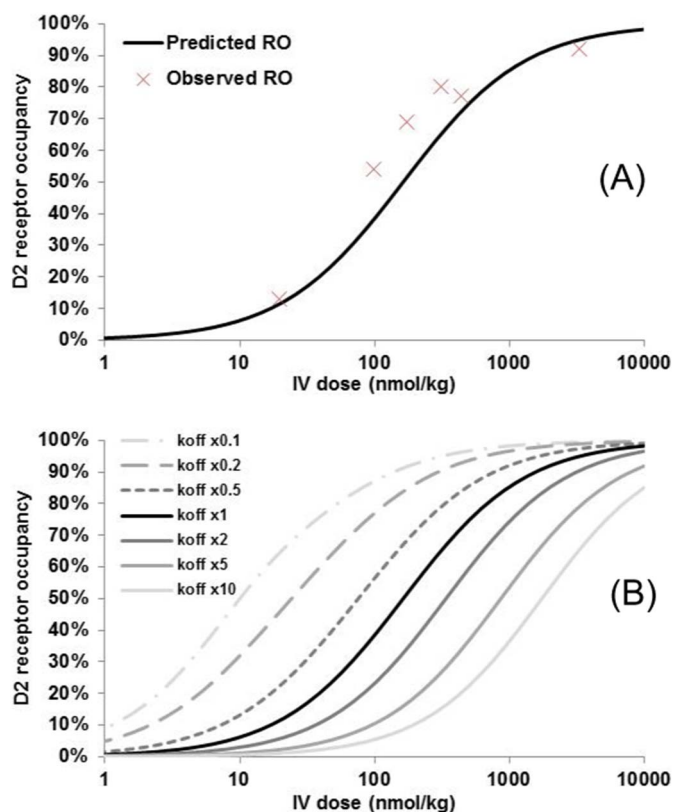
**Fig. 6.** Prediction of striatum D2 receptor occupancy after IV raclopride administration. A) Dose-RO relationship. Observed data were from Köhler and Boethius, at t = 75 min. B) The effect of changing $k_{off}$ from the original value of 0.165 $min^{-1}$ ($k_{on}$ kept constant at 0.049 $nM^{-1}$ $min^{-1}$) on the simulated RO. The simulation setting was also based on the study of from Köhler and Boethius, at t = 75 min.



**Fig. 7.** Prediction of striatum D2 receptor occupancy after subcutaneous raclopride administration. A) Dose-RO relationship. Observed data were from Wadenberg et al. and Marcus et al., at t = 60 min. B) RO-time profile. Observed data were from Wadenberg et al., 2000, at 5760 nmol/kg.

dosing, which are currently not available in literature. An example of Berkeley Madonna code for PK and D2 RO simulation is provided in the Supplementary material. The advantages of the LC − MS based approach are further discussed in Sections 4.2 and 4.3.

### 4.2. Advantages of the "non-radiolabeled tracer with LC − MS quantification" approach

When used as an *in vivo* tracer in animals, raclopride is usually administered as radiolabeled [3H]-raclopride (or as [11C]-raclopride in PET) with subsequent radioactivity measurement; however, an alternative approach that combines non-radiolabeled raclopride and LC − MS quantification is gaining momentum in recent years. This is first reported is by Barth and her colleagues (Barth et al., 2006; Chernet et al., 2005), who used non-radiolabeled raclopride at a sub-pharmacological dose (IV 6 nmol/kg, estimated RO ≈ 20%, Fig. 5) as a D2 tracer in rats, and the striatum and cerebellum tissue concentrations were quantified by LC − MS. The striatum D2 RO values of eight antipsychotic drugs measured with this non-radiolabeled raclopride were very comparable to those with the traditional [3H]-raclopride tracer (tracer dose, 0.4 nmol/kg, IV). Since then this approach has been adopted by other research groups, for instance in (Hutson et al., 2016; Nirogi et al., 2013). Since most the drugs and tracers that act on the central nervous system (including raclopride) are relatively lipophilic and are extensively metabolized (Wong et al., 2012), LC − MS allows unambiguous and simultaneous quantification of the drug, tracer and their (active) metabolites in one single sample, which is not feasible with radioactivity counting. Moreover, the limitations related to radiochemical synthesis and radioactivity hazard could be avoided. Furthermore, variation in specific activity of [11C]-raclopride, and hence the amount of cold raclopride co-administered, could lead to
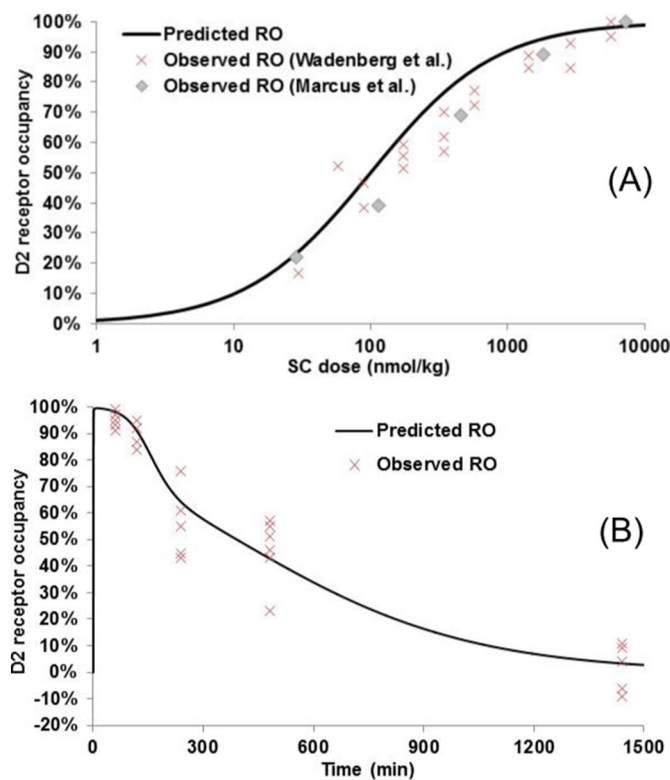
variation in the PET imaging outcomes such as binding potential (Hume et al., 1992). In contrast, for non-radiolabeled tracer the amount of raclopride administered should be more uniform and accurate. Last but not least, the short 20-min decay half-life of [11C] restricts the collection of tracer kinetics data to only 1 h post-dose, while with non-radiolabeled tracers data could be collected over an extended period of time (*e.g.* 10 h in the current study, and 24 h in (Suresh et al., 2011)), which could provide a more complete dataset for subsequent data analysis and modeling.

In summary, the LC − MS approach can facilitate the development of new tracers and drugs, especially in the early development stages such that the PK and RO time profiles of potential tracer/drug candidates can already be characterized with the easily accessible LC − MS before investing resources into radio-labeling and PET/SPECT imaging. It is expected that such "non-radiolabeled tracer with LC − MS" approach will be increasingly adopted for both fundamental research and drug development, and our PK-RO model will be useful for rat studies that involve the administration of raclopride as D2 tracer.

Despite the aforementioned advantages of this LC − MS approach, it should be emphasized that PET imaging remains the desired approach in certain pharmacological studies. PET imaging is less invasive and allows multiple measurements in the same animal, which is crucial for longitudinal studies and evaluation of repeated drug or non-drug interventions. Moreover, since radioactivity detection is more sensitive to LC − MS quantification, the dose of raclopride tracer needed is lower for radiolabeled raclopride, which would reduce the potential interferences to the outcomes due to the pharmacological actions of the tracer itself. By analyzing the PET data with suitable modeling approach (considering for example the plasma input function, time-profile of radio-metabolite, reference tissue model, *etc.*) (Dupont and Warwick, 2009), some of the shortcomings of small-animal PET imaging mentioned in Sections 4.2 and 4.3 could be compensated. Indeed, the striatum binding potential obtained in [11C]-raclopride in non-

anesthetized humans was just comparable to those in anesthetized rats and mice when the PET data was analyzed using the reference tissue model (Kuntner, 2014), even though the metabolic conversion of [$^{11}$C]-raclopride to radio-metabolite is much slower in humans (Alexoff et al., 1995) than in rodents (Hume et al., 1992; Patel et al., 2008).

### 4.3. Predicting raclopride PK and RO in anesthetized rats/restrained rats in PET studies

It is important to mention that this PK-RO model was constructed based on non-anesthetized, freely moving rats, and it might not be applicable for the prediction of rats under anesthesia and/or restrain which have profound impact on raclopride PK and RO. For conventional PET imaging in rats or mice, anesthesia or complete restraint is generally required to prevent motion artifact during imaging. Isoflurane, an anesthetic commonly used in rodent PET imaging studies, significantly increases the uptake of IV [$^{3}$H]-raclopride to rat striatum and cerebellum by 40% (McCormick et al., 2011). Ketamine plus xylazine anesthesia also increases IV [$^{11}$C]-raclopride rat brain uptake by five-fold regardless of the brain region (Patel et al., 2008), which could be partly due to the suppressive effect of ketamine/xylazine on systemic clearance (Wong et al., 2014). Consequently, the IV raclopride dose needed to occupy 50% of striatum D2 receptors in [$^{11}$C]-raclopride PET studies with anesthetized rats ranged from 6 nmol/kg (Schiffer et al., 2005) to 9 nmol/kg (Opacka-Juffry et al., 1998) to 17 nmol/kg (Hume et al., 1995). These were much lower than the required dose estimated from the current study (Fig. 6) and a previous study (Köhler and Karlsson-Boethius, 1988) with non-anesthetized rats (both around 100 nmol/kg), indicating that the effect of anesthesia on raclopride kinetics is significant. Different anesthetics also differentially alter the activity and dopamine turnover of dopaminergic neurons (Müller et al., 2011), which would, in turn, alter the D2 RO of raclopride. On the other hand, restraining a non-anesthetized rodent would decrease the binding of [$^{11}$C]-raclopride in striatum (Patel et al., 2008; Takuwa et al., 2015), which is partly due to the immobility stress-induced dopamine released and displacement of [$^{11}$C]-raclopride.

Encouragingly, thanks to advance in mechanical and computational engineering, raclopride PET imaging in rodents without the need of anesthesia is in active development. Devices that allow [$^{11}$C]-raclopride brain imaging of non-anesthetized rodents that are freely walking with minimal restrain have been developed (Schulz et al., 2011; Takuwa et al., 2015). Besides PET imaging, an alternative approach would be the use of intracerebral microprobe that is sensitive to beta emission from [$^{11}$C]-raclopride. A chronically implanted wireless pixelated beta-microprobe was recently developed to measure the time-activity curves of [$^{11}$C]-raclopride in non-anesthetized, freely moving rats, and the specific binding in striatum was significantly lower than those in isoflurane-anesthetized rats (Balasse et al., 2015). Therefore, imaging in non-anesthetized rats is indeed feasible and in that case our PK-RO model would be applicable.

### 4.4. Modeling raclopride PK and RO: current approach versus PET imaging approach

In the current study, the *in vivo* data were analyzed by population (nonlinear mixed effect) modeling to estimate PK (*e.g.* clearance between body compartments) and receptor binding parameters ($K_d$). This modeling approach has several advantages (Liefaard et al., 2005). It is possible to model all data from all rats simultaneously (*e.g.* data from different studies, at different doses), resulting in better statistical power for estimation of the parameters of interest that would otherwise be difficult to quantify. Also, individuals with an incomplete dataset can be included in the analysis. Finally, it is possible to estimate inter-individual variability of different structural parameters. The population approach has been previously applied to the characterization of the brain kinetics and RO of radiotracers from both small animal (Liefaard

et al., 2005) and human (Kågedal et al., 2012) PET data. Our current study demonstrated that such approach could also be applied to non-radiolabeled tracers.

Hume et al. (Hume et al., 1992) fitted their PET imaging data of a single-dose [$^{11}$C]-raclopride in anesthetized rats into a four-compartment reference tissue model. The ratio between the rate constants of raclopride uptake from the plasma compartment into striatum and cerebellum ranged from 0.72 to 1.0. In our PK-RO model the rate constants for striatum uptake (Q2/V2 = 0.069) and cerebellum uptake (Q3/V3 = 0.082) gave a similar ratio of 0.84, again suggesting that the uptake rate into striatum was slower than that into cerebellum. Nevertheless, Hume et al. stated that the brain uptake values from individual rats varied considerably and the fitted rate constants had relatively large associated errors. Inter-individual variability was also observed in the current study and some parameter estimates in our PK-RO model showed certain degree of uncertainty (Table 3). It is worth mentioning that the radio-metabolites of [$^{11}$C]-raclopride does not enter the rat brain tissue (Hume et al., 1992; Köhler et al., 1985) and therefore only the plasma input function needed to be corrected for the metabolites when modeling the PET data. For other radiotracers, it is necessary to characterize the metabolites. If the contribution of the radioactive metabolite at the tissue of interest cannot be neglected it should be incorporated into the model (Dupont and Warwick, 2009).

In addition to the PET imaging technique, kinetics parameters of [$^{11}$C]-raclopride had also been estimated in anesthetized rats with the beta-microprobe technique. With a multi-injection protocol, Mauger et al. (Mauger et al., 2005) fitted the radioactivity data detected by the intracerebral microprobe into a three-compartment model. The ratio between the rate constants of raclopride uptake from into striatum and cerebellum was 0.82, similar to those estimated by us and by (Hume et al., 1992). Their estimated $k_{off}$ was 0.20 min$^{-1}$, while ours was 0.17 min$^{-1}$. Their estimated $B_{max}$ was 20 nM, which was close to the value we used (25 nM). Therefore, while our approach (LC − MS based approach with non-radiolabeled raclopride, data fitted into population modeling) differed from those adopted by (Hume et al., 1992) and (Mauger et al., 2005) (radioactivity based approach with [$^{11}$C]-raclopride, non-population modeling), comparable parameter estimates were achieved, which supported the utility of our proposed approach.

### 4.5. Predicting raclopride PK and RO after repeated raclopride dosing

While the developed model could predict the PK and RO outcomes after a single-dose of raclopride, whether it could also predict the outcomes after repeated dosing remains to be explored. Ericson et al. suggested that when raclopride was given repeatedly to rat, the plasma concentration would increase with time, although no further information was provided by the authors (Ericson et al., 1996). Self-inhibition of metabolism *via* downregulation of CYP enzymes could be an explanation. In rats, subchronic systemic administration of selective D2 antagonists such as raclopride and other similar benzamides sulpiride and remoxipride could suppress the expression and activity of liver CYP 1A, 1B, 2B, 2C and 3A isozymes (Harkitis et al., 2015; Jurica et al., 2011; Rane et al., 1996), while repeated intracerebral raclopride administration increases CYP 2C activity (Sabová et al., 2013). In addition to modifying systemic PK, chronic administration of raclopride (*via* subcutaneous osmotic pump) also increases [$^{3}$H]-raclopride binding sites in rat striatum (See et al., 1990). In other words, certain PK (*e.g.* systemic clearance) and D2-binding ($B_{max}$, $K_d$) parameters need to be changed in the repeated dosing setting.

### 4.6. The role of in vitro binding kinetics values in predicting in vivo D2 RO

The *in vivo* $K_d$ value estimated by the current PK-RO model (3.4 nM) is higher than the average $K_d$ values from *in vitro* studies that measured raclopride-D2 binding kinetics with rat striatum homogenate (≈ 1.1 nM) (Cumming, 2011). If our estimated $K_d$ is valid, then the

lower affinity *in vivo* could be, at least partly, explained by the presence of endogenous dopamine. The basal level of extra-synaptic dopamine in rat striatum ECF is estimated to be $20 - 100$ nM (Fisher et al., 1995; Schiffer et al., 2005). Administration of D2 receptor antagonist such as raclopride would increase dopamine turnover and dopamine release, and after a high IV raclopride dose (D2 RO > 90%) dopamine concentration in rat striatum ECF would increase by 300% (Schiffer et al., 2005). Dopamine concentration inside the synapse is expected to be even higher, probably up to $100 - 200$ nM (Laruelle, 2012). The inhibition constant of dopamine on [$^3$H]-raclopride binding to high-affinity state D2 receptors in rat striatum homogenate is around 20 nM (Dewar et al., 1989; Hall et al., 1990), well below the dopamine concentration available and thus competitive inhibition is likely *in vivo*. Indeed, among the commonly applied D2 antagonist tracers, raclopride is suggested to be most sensitive to displacement by endogenous dopamine (Morris and Yoder, 2007). Dopamine not only competes with raclopride for the D2 binding sites, but also induces long-lasting internalization of D2 receptors from plasma membrane into intracellular environment. Since raclopride has a lower affinity for internalized receptors compared to receptor expressed at cell surface, this might also contribute to the discrepancy between *in vivo* and *in vitro* $K_d$ values (Laruelle, 2012).

Binding kinetic parameters ($K_d$, $k_{off}$, and $k_{on}$) measured in *in vitro* studies are also dependent on the experimental settings (de Witte et al., 2016). For instance, in rat striatum tissue homogenate the $K_d$ values of [$^3$H]-raclopride to D2 receptors maintained between 1.6 nM to 1.8 nM when the incubation temperature increased from 15 °C to 30 °C; however, $K_d$ raised to 3.0 nM when the temperature further increased to 37 °C (Hall et al., 1988). To accurately predict the RO, it is crucial to adopt an integrative approach that combines well-designed (*i.e.* physiologically relevant) *in vitro* binding studies and mathematical models that describe the relevant *in vivo* processes (*e.g.* the effect of endogenous ligand and receptor internalization) governing drug-receptor binding. Interested readers are referred to recent reviews by (de Witte et al., 2016) and (Schuetz et al., 2017) for details.

In addition to D2 receptor, raclopride also binds to D3 receptor *in vitro* with comparable $K_d$ (Seeman, 2011). Nevertheless, in striatum the density of D3 receptor is at least several folds lower than that of D2 receptor, particularly for young rats (< 0.25 kg) (Hillefors et al., 1999; Levant, 1998). Moreover, antipsychotics such as olanzapine, risperidone and clozapine, when administered to non-anesthetized rats at clinically-relevant doses (D2 RO around 80%) occupy far smaller proportion of D3 receptors (D3 RO < 40%) *in vivo* (McCormick et al., 2013) than would be predicted by their *in vitro* affinities (*i.e.* comparable $K_d$ at D2 and D3 (Seeman, 2011)). Therefore, raclopride binding to D3 receptors should not have a quantitatively important contribution to the total uptake measured in the striatum.

### 4.7. Summary

The present study, together with previous research, shows that raclopride possesses most of the criteria required for a successful tracer for drug targets in brain: for example, $B_{max}/K_d$ > 5–10, $f_{u,brain}$ > 0.01–0.05, log $P$ within 1 to 5, and rapid permeation across blood-brain barrier without the involvement of active transport (Need et al., 2017). In addition, the relatively fast $k_{on}$ and $k_{off}$ rates shorten the time needed to reach equilibrium receptor binding, which is inversely proportional to ($k_{on}$ × [raclopride concentration] + $k_{off}$) (Guo et al., 2015). It is expected that raclopride will continue to be one of the most commonly used *in vivo* tracers for D2 investigations, and our PK-RO model will be useful when designing these pharmacological studies. The model could be used not just for selecting the optimal dose amount, but also for selecting the optimal dosing method (for instance, the duration of the IV infusion and the dosing time of raclopride relative to the intervention being investigated, *e.g.* a drug challenge) in order to achieve the desired D2 RO level at a certain time period.

## 5. Conclusion

A predictive model describing the quantitative relationship between dose, PK and D2 RO of raclopride in non-anesthetized rat was established. This PK-RO model could accurately predict the plasma PK, brain tissue PK and striatum D2 RO after IV raclopride dosing. Further extension of this model for predicting D2 RO after subcutaneous raclopride administration has been shown to be possible, although this should be further validated with additional subcutaneous PK data. The developed PK-RO model could facilitate the selection of optimal dose and dosing time when raclopride is used as tracer or as pharmacological intervention in various rat studies. This study also demonstrated that the LC − MS based approach might complement the imaging-based approach in evaluating the systemic disposition and brain kinetics of tracers and facilitate the development of novel tracers.

## Appendix A. Supplementary data

Supplementary data to this article can be found online at https://doi.org/10.1016/j.ejps.2017.10.031.

## References

Alexoff, D.L., Shea, C., Fowler, J.S., King, P., Gatley, S.J., Schlyer, D.J., Wolf, A.P., 1995. Plasma input function determination for PET using a commercial laboratory robot. Nucl. Med. Biol. 22, 893–904.

Baciu, M., Sebai, S.C., Ces, O., Mulet, X., Clarke, J.A., Shearman, G.C., Law, R.V., Templer, R.H., Plisson, C., Parker, C.A., Gee, A., 2006. Degradative transport of cationic amphiphilic drugs across phospholipid bilayers. Philos. Trans. R. Soc. A Math. Phys. Eng. Sci. 364, 2597–2614.

Balasse, L., Maerk, J., Pain, F., Genoux, A., Fieux, S., Lefebvre, F., Morel, C., Gisquet-Verrier, P., Lanièce, P., Zimmer, L., 2015. PIXSIC: a wireless intracerebral radio-sensitive probe in freely moving rats. Mol. Imaging 14, 484–489.

Barth, V.N., Chernet, E., Martin, L.J., Need, A.B., Rash, K.S., Morin, M., Phebus, L.A., 2006. Comparison of rat dopamine D2 receptor occupancy for a series of antipsychotic drugs measured using radiolabeled or nonlabeled raclopride tracer. Life Sci. 78, 3007–3012.

Bosch, R., vanLierop, M.-J., deKam, P.-J., Kruithof, A.C., Burggraaf, J., deGreef, R., Visser, S.A.G., Johnson-Levonas, A.O., Kleijn, H.-J., 2016. A PK-PD model-based assessment of sugammadex effects on coagulation parameters. Eur. J. Pharm. Sci. 84, 9–17.

van den Brink, W.J., Wong, Y.C., Gülave, B., van der Graaf, P.H., de Lange, E.C.M., 2017. Revealing the neuroendocrine response after remoxipride treatment using multi-biomarker discovery and quantifying it by PK/PD modeling. AAPS J. 19, 274–285.

Casey, D., Charalambous, K., Gee, A., Law, R.V., Ces, O., 2014. Amphiphilic drug interactions with model cellular membranes are influenced by lipid chain-melting temperature. J. R. Soc. Interface 11 (20131062).

Chernet, E., Martin, L.J., Li, D., Need, A.B., Barth, V.N., Rash, K.S., Phebus, L.A., 2005. Use of LC/MS to assess brain tracer distribution in preclinical, in vivo receptor occupancy studies: dopamine D2, serotonin 2A and NK-1 receptors as examples. Life Sci. 78, 340–346.

Cumming, P., 2011. Absolute abundances and affinity states of dopamine receptors in mammalian brain: a review. Synapse 65, 892–909.

Dewar, K.M., Montreuil, B., Grondin, L., Reader, T.A., 1989. Dopamine D2 receptors labeled with [3H]raclopride in rat and rabbit brains. Equilibrium binding, kinetics, distribution and selectivity. J. Pharmacol. Exp. Ther. 250, 696–706.

Dupont, P., Warwick, J., 2009. Kinetic modelling in small animal imaging with PET. Methods 48, 98–103.

Ericson, H., Radesäter, A.C., Servin, E., Magnusson, O., Mohringe, B., 1996. Effects of intermittent and continuous subchronic administration of raclopride on motor activity, dopamine turnover and receptor occupancy in the rat. Pharmacol. Toxicol. 79, 277–286.

Farde, L., Hall, H., Ehrin, E., Sedvall, G., 1986. Quantitative analysis of D2 dopamine receptor binding in the living human brain by PET. Science 231, 258–261.

Fisher, R.E., Morris, E.D., Alpert, N.M., Fischman, A.J., 1995. In vivo imaging of

neuromodulatory synaptic transmission using PET: a review of relevant neurophysiology. Hum. Brain Mapp. 3, 24–34.

Guo, D., IJzerman, A.P., Heitman, L.H., 2015. Importance of drug–target residence time at G protein-coupled receptors – a case for the adenosine receptors. In: Keserü, G.M., Swinney, D.C. (Eds.), Thermodynamics and Kinetics of Drug Binding. Wiley-VCH Verlag GmbH & Co. KGaA, pp. 257–272.

Hall, H., Wedel, I., Sallemark, M., 1988. Effects of temperature on the in vitro binding of 3H-raclopride to rat striatal dopamine-D2 receptors. Pharmacol. Toxicol. 63, 118–121.

Hall, H., Wedel, I., Halldin, C., Kopp, J., Farde, L., 1990. Comparison of the in vitro receptor binding properties of *N*-[3H]methylspiperone and [3H]raclopride to rat and human brain membranes. J. Neurochem. 55, 2048–2057.

Harkitis, P., Daskalopoulos, E.P., Malliou, F., Lang, M.A., Marselos, M., Fotopoulos, A., Albucharali, G., Konstandi, M., 2015. Dopamine D2-receptor antagonists down-regulate CYP1A1/2 and CYP1B1 in the rat liver. PLoS One 10 (e0128708).

Hillefors, M., vonEuler, M., Hedlund, P.B., vonEuler, G., 1999. Prominent binding of the dopamine D3 agonist [3H]PD 128907 in the caudate-putamen of the adult rat. Brain Res. 822, 126–131.

Hume, S.P., Myers, R., Bloomfield, P.M., Opacka-Juffry, J., Cremer, J.E., Ahier, R.G., Luthra, S.K., Brooks, D.J., Lammertsma, A.A., 1992. Quantitation of carbon-11-labeled raclopride in rat striatum using positron emission tomography. Synapse 12, 47–54.

Hume, S.P., Opacka-Juffry, J., Myers, R., Ahier, R.G., Ashworth, S., Brooks, D.J., Lammertsma, A.A., 1995. Effect of L-dopa and 6-hydroxydopamine lesioning on [11C]raclopride binding in rat striatum, quantified using PET. Synapse 21, 45–53.

Hutson, P.H., Rowley, H.L., Gosden, J., Kulkarni, R.S., Slater, N., Love, P.L., Wang, Y., Heal, D., 2016. The effects in rats of lisdexamfetamine in combination with olanzapine on mesocorticolimbic dopamine efflux, striatal dopamine D2 receptor occupancy and stimulus generalization to a d-amphetamine cue. Neuropharmacology 101, 24–35.

Joshi, E.M., Need, A., Schaus, J., Chen, Z., Benesh, D., Mitch, C., Morton, S., Raub, T.J., Phebus, L., Barth, V., 2014. Efficiency gains in tracer identification for nuclear imaging: can in vivo LC-MS/MS evaluation of small molecules screen for successful PET tracers? ACS Chem. Neurosci. 5, 1154–1163.

Jurica, J., Zendulka, O., Trubač, R., Šulcová, A., 2011. Systemic administration of D2 antagonist raclopride inhibits CYP1A2 in the rat model of isolated perfused liver. Act. Nerv. Super. Rediviva 53, 32–34.

Kågedal, M., Cselényi, Z., Nyberg, S., Jönsson, S., Raboisson, P., Stenkrona, P., Hooker, A.C., Karlsson, M.O., 2012. Non-linear mixed effects modelling of positron emission tomography data for simultaneous estimation of radioligand kinetics and occupancy in healthy volunteers. NeuroImage 61, 849–856.

Knibbe, C.A.J., Zuideveld, K.P., Aarts, L.P.H.J., Kuks, P.F.M., Danhof, M., 2005. Allometric relationships between the pharmacokinetics of propofol in rats, children and adults. Br. J. Clin. Pharmacol. 59, 705–711.

Köhler, C., Karlsson-Boethius, G., 1988. In vivo labelling of rat brain dopamine D-2 receptors. Stereoselective blockade by the D-2 antagonist raclopride and its enantiomer of 3H-spiperone, 3H-*N*,*N*-propylnorapomorphine and 3H-raclopride binding in the rat brain. J. Neural Transm. Vol. 73, 87–100.

Köhler, C., Hall, H., Ogren, S.O., Gawell, L., 1985. Specific in vitro and in vivo binding of 3H-raclopride. A potent substituted benzamide drug with high affinity for dopamine D-2 receptors in the rat brain. Biochem. Pharmacol. 34, 2251–2259.

Kozielska, M., Johnson, M., Pilla Reddy, V., Vermeulen, A., Li, C., Grimwood, S., deGreef, R., Groothuis, G.M.M., Danhof, M., Proost, J.H., 2012. Pharmacokinetic-pharmacodynamic modeling of the D2 and 5-HT2A receptor occupancy of risperidone and paliperidone in rats. Pharm. Res. 29, 1932–1948.

Kuntner, C., 2014. Kinetic modeling in preclinical positron emission tomography. Z. Med. Phys. 24, 274–285.

de Lange, E.C., 2013. The mastermind approach to CNS drug therapy: translational prediction of human brain distribution, target site kinetics, and therapeutic effects. Fluids Barriers CNS 10, 12.

Laruelle, M., 2012. Measuring dopamine synaptic transmission with molecular imaging and pharmacological challenges: the state of the art. In: Gründer, G. (Ed.), Molecular Imaging in the Clinical Neurosciences. Humana Press, Totowa, NJ, pp. 163–203.

Levant, B., 1998. Differential distribution of D3 dopamine receptors in the brains of several mammalian species. Brain Res. 800, 269–274.

Liefaard, L.C., Ploeger, B.A., Molthoff, C.F.M., Boellaard, R., Lammertsma, A.A., Danhof, M., Voskuyl, R.A., 2005. Population pharmacokinetic analysis for simultaneous determination of B max and K D in vivo by positron emission tomography. Mol. Imaging Biol. 7, 411–421.

Linnér, L., Wiker, C., Wadenberg, M.L., Schalling, M., Svensson, T.H., 2002. Noradrenaline reuptake inhibition enhances the antipsychotic-like effect of raclopride and potentiates D2-blockage–induced dopamine release in the medial prefrontal cortex of the rat. Neuropsychopharmacology 27, 691–698.

Loryan, I., Fridén, M., Hammarlund-Udenaes, M., 2013. The brain slice method for studying drug distribution in the CNS. Fluids Barriers CNS 10, 6.

Marcus, M., Jardemark, K., Wadenberg, M., Langlois, X., Hertel, P., Svensson, T., 2005. Combined α2 and D2/3 receptor blockade enhances cortical glutamatergic transmission and reverses cognitive impairment in the rat. Int. J. Neuropsychopharmacol. 8, 315–327.

Mauger, G., Saba, W., Hantraye, P., Dolle, F., Coulon, C., Bramoullé, Y., Chalon, S., Greégoire, M.-C., 2005. Multiinjection approach for D 2 receptor binding quantification in living rats using [11C]raclopride and the β-microprobe: crossvalidation with in vitro binding data. J. Cereb. Blood Flow Metab. 25, 1517–1527.

McCormick, P.N., Ginovart, N., Wilson, A.A., 2011. Isoflurane anaesthesia differentially affects the amphetamine sensitivity of agonist and antagonist D2/D3 positron emission tomography radiotracers: implications for in vivo imaging of dopamine release.

Mol. Imaging Biol. 13, 737–746.

McCormick, P.N., Wilson, V.S., Wilson, A.A., Remington, G.J., 2013. Acutely administered antipsychotic drugs are highly selective for dopamine D2 over D3 receptors. Pharmacol. Res. 70, 66–71.

Mengler, L., Khmelinskii, A., Diedenhofen, M., Po, C., Staring, M., Lelieveldt, B.P.F., Hoehn, M., 2014. Brain maturation of the adolescent rat cortex and striatum: changes in volume and myelination. NeuroImage 84, 35–44.

Morris, E.D., Yoder, K.K., 2007. Positron emission tomography displacement sensitivity: predicting binding potential change for positron emission tomography tracers based on their kinetic characteristics. J. Cereb. Blood Flow Metab. 27, 606–617.

Müller, C.P., Pum, M.E., Amato, D., Schüttler, J., Huston, J.P., Silva, M.A.D.S., 2011. The in vivo neurochemistry of the brain during general anesthesia. J. Neurochem. 119, 419–446.

Need, A., Kant, N., Jesudason, C., Barth, V., 2017. Approaches for the discovery of novel positron emission tomography radiotracers for brain imaging. Clin. Transl. Imaging 5, 265–274.

Nirogi, R., Kandikere, V., Jayarajan, P., Bhyrapuneni, G., Saralaya, R., Muddana, N., Abraham, R., 2013. Aripiprazole in an animal model of chronic alcohol consumption and dopamine D 2 receptor occupancy in rats. Am. J. Drug Alcohol Abuse 39, 72–79.

Opacka-Juffry, J., Ashworth, S., Ahier, R.G., Hume, S.P., 1998. Modulatory effects of L-DOPA on D2 dopamine receptors in rat striatum, measured using in vivo microdialysis and PET. J. Neural Transm. 105, 349.

Packeu, A., Wennerberg, M., Balendran, A., Vauquelin, G., 2010. Estimation of the dissociation rate of unlabelled ligand-receptor complexes by a "two-step" competition binding approach. Br. J. Pharmacol. 161, 1311–1328.

Patel, V.D., Lee, D.E., Alexoff, D.L., Dewey, S.L., Schiffer, W.K., 2008. Imaging dopamine release with positron emission tomography (PET) and (11)C-raclopride in freely moving animals. NeuroImage 41, 1051–1066.

Rane, A., Liu, Z., Levol, R., Bjelfman, C., Thyr, C., Ericson, H., Hansson, T., Henderson, C., Wolf, C.R., 1996. Differential effects of neuroleptic agents on hepatic cytochrome P-450 isozymes in the male rat. Biochim. Biophys. Acta 1291, 60–66.

Sabová, M., Zendulka, O., Jurica, J., Dovrtelová, G., Šulcová, A., 2013. Differential role of central and peripheral D2 receptors in the regulation of CYP metabolic activity. 10th International ISSX Meeting.

Schiffer, W.K., Alexoff, D.L., Shea, C., Logan, J., Dewey, S.L., 2005. Development of a simultaneous PET/microdialysis method to identify the optimal dose of 11C-raclopride for small animal imaging. J. Neurosci. Methods 144, 25–34.

Schuetz, D.A., de Witte, W.E.A., Wong, Y.C., Knasmueller, B., Richter, L., Kokh, D.B., Sadiq, S.K., Bosma, R., Nederpelt, I., Heitman, L.H., Segala, E., Amaral, M., Guo, D., Andres, D., Georgi, V., Stoddart, L.A., Hill, S., Cooke, R.M., DeGraaf, C., Leurs, R., Frech, M., Wade, R.C., de Lange, E.C.M., IJzerman, A.P., Müller-Fahrnow, A., Ecker, G.F., 2017. Kinetics for Drug Discovery: an industry-driven effort to target drug residence time. Drug Discov. Today 22, 896–911.

Schulz, D., Southekal, S., Junnarkar, S.S., Pratte, J.-F., Purschke, M.L., Stoll, S.P., Ravindranath, B., Maramraju, S.H., Krishnamoorthy, S., Henn, F.A., O'Connor, P., Woody, C.L., Schlyer, D.J., Vaska, P., 2011. Simultaneous assessment of rodent behavior and neurochemistry using a miniature positron emission tomograph. Nat. Methods 8, 347–352.

See, R.E., Toga, A.W., Ellison, G., 1990. Autoradiographic analysis of regional alterations in brain receptors following chronic administration and withdrawal of typical and atypical neuroleptics in rats. J. Neural Transm. Gen. Sect. 82, 93–109.

Seeman, P., 2011. All roads to schizophrenia lead to dopamine supersensitivity and elevated dopamine D2high receptors. CNS Neurosci. Ther. 17, 118–132.

Stevens, J., Suidgeest, E., van der Graaf, P.H., Danhof, M., de Lange, E.C.M., 2009. A new minimal-stress freely-moving rat model for preclinical studies on intranasal administration of CNS drugs. Pharm. Res. 26, 1911–1917.

Stevens, J., van den Berg, D.-J., de Ridder, S., Niederländer, H.A.G., van der Graaf, P.H., Danhof, M., de Lange, E.C.M., 2010. Online solid phase extraction with liquid chromatography–tandem mass spectrometry to analyze remoxipride in small plasma-, brain homogenate-, and brain microdialysate samples. J. Chromatogr. B 878, 969–975.

Summerfield, S.G., Lucas, A.J., Porter, R.A., Jeffrey, P., Gunn, R.N., Read, K.R., Stevens, A.J., Metcalf, A.C., Osuna, M.C., Kilford, P.J., Passchier, J., Ruffo, A.D., 2008. Toward an improved prediction of human in vivo brain penetration. Xenobiotica 38, 1518–1535.

Suresh, P.S., Punde, R.R., Gupta, M., Dixit, A., Giri, S., Rajagopal, S., Mullangi, R., Mullangi, R., 2011. A highly sensitive LC-MS/MS method for the determination of S-raclopride in rat plasma: application to a pharmacokinetic study in rats. Biomed. Chromatogr. 25, 930–937.

Takuwa, H., Maeda, J., Ikoma, Y., Tokunaga, M., Wakizaka, H., Uchida, S., Kanno, I., Taniguchi, J., Ito, H., Higuchi, M., 2015. [11C]Raclopride binding in the striatum of minimally restrained and free-walking awake mice in a positron emission tomography study. Synapse 69, 600–606.

Wadenberg, M.-L.G., 2010. Conditioned avoidance response in the development of new antipsychotics. Curr. Pharm. Des. 16, 358–370.

Wadenberg, M.L.G., Kapur, S., Soliman, A., Jones, C., Vaccarino, F., 2000. Dopamine D2 receptor occupancy predicts catalepsy and the suppression of conditioned avoidance response behaviour in rats. Psychopharmacology 150, 422–429.

Westerhout, J., Ploeger, B., Smeets, J., Danhof, M., deLange, E.C.M., 2012. Physiologically based pharmacokinetic modeling to investigate regional brain distribution kinetics in rats. AAPS J. 14, 543–553.

Westerhout, J., Smeets, J., Danhof, M., de Lange, E.C.M., 2013. The impact of P-gp functionality on non-steady state relationships between CSF and brain extracellular fluid. J. Pharmacokinet. Pharmacodyn. 40, 327–342.

de Witte, W.E., Wong, Y.C., Nederpelt, I., Heitman, L.H., Danhof, M., van der Graaf, P.H., Gilissen, R.A., de Lange, E.C.M., 2016. Mechanistic models enable the rational use of

in vitro drug-target binding kinetics for better drug effects in patients. Expert Opin. Drug Discovery 11, 45–63.

Wong, Y.C., Zuo, Z., 2013. Brain disposition and catalepsy after intranasal delivery of loxapine: role of metabolism in PK/PD of intranasal CNS drugs. Pharm. Res. 30, 2368–2384.

Wong, Y.C., Qian, S., Zuo, Z., 2012. Regioselective biotransformation of CNS drugs and its clinical impact on adverse drug reactions. Expert Opin. Drug Metab. Toxicol. 8, 833–854.

Wong, Y.C., Qian, S., Zuo, Z., 2014. Pharmacokinetic comparison between the long-term anesthetized, short-term anesthetized and conscious rat models in nasal drug delivery. Pharm. Res. 31, 2107–2123.

Yamamoto, Y., Välitalo, P.A., van den Berg, D.-J., Hartman, R., van den Brink, W., Wong, Y.C., Huntjens, D.R., Proost, J.H., Vermeulen, A., Krauwinkel, W., Bakshi, S., Aranzana-Climent, V., Marchand, S., Dahyot-Fizelier, C., Couet, W., Danhof, M., van Hasselt, J.G.C., de Lange, E.C.M., 2017. A generic multi-compartmental CNS distribution model structure for 9 drugs allows prediction of human brain target site concentrations. Pharm. Res. 34, 333–351.